Bond and site defects in fully frustrated two-dimensional Ising systems

1997 J. Phys. A: Math. Gen. 30 2947

(http://iopscience.iop.org/0305-4470/30/9/010)

J. Phys. A: Math. Gen. **30** (1997) 2947–2962. Printed in the UK PII: S0305-4470(97)78237-4

Bond and site defects in fully frustrated two-dimensional Ising systems

J R Gonçalves†, J Poulter‡ and J A Blackman†

† Department of Physics, University of Reading, Whiteknights, PO Box 220, Reading RG6 6AF, UK

‡ Department of Mathematics, Faculty of Science, Mahidol University, Bangkok 10400, Thailand

Received 30 September 1996

Abstract. The Villain model and the triangular antiferromagnet are the two canonical fully frustrated two-dimensional Ising systems. Exact results are presented for the entropy changes that occur when bond and site defects are introduced into these systems. The results for single defects are obtained first. Pairs of site defects are then discussed. The change in entropy is evaluated to the leading term in an expansion in powers of R^{-1} where R is the separation of the defects. The entropy shift is $\sim R^{-2}$ in both models except for special values of R in the Villain model where it is $\sim R^{-4}$.

1. Introduction

The purpose of this paper is to present some exact results for the entropy changes brought about in two-dimensional (2D) fully frustrated Ising systems by the introduction of simple defects. These results have a relevance to a particular line of research in spin glasses. To put the current work into context, we begin with a very brief summary of the spin glass investigations, although specifically spin glass issues are not the concern of this paper.

Spin glasses are characterized by frustration and randomness. There have been a number of studies that have sought to introduce randomness into initially non-random frustrated systems by means of defects. Triangular (2D) and fcc (3D) antiferromagnetic lattices are popular systems to use. The starting models are fully frustrated with a highly degenerate ground state and the replacement of magnetic sites with a non-magnetic species reduces frustration but inserts randomness.

The presence of defects reduces the entropy of the fully frustrated system and early Monte Carlo (MC) calculations [1] give some indication that even in the site-diluted triangular antiferromagnet some type of long-range order was possible. The slowing down associated with MC calculations in systems of this sort make it notoriously difficult to draw firm conclusions about the low-temperature behaviour, however, and renormalization group work [2] gave no indications of the freezing in of long-range order; this is consistent with the assumed lower critical dimensionality of three for a spin glass. More recent MC calculations [3] and transfer matrix methods [4] have attempted to monitor the entropy as a function of defect concentration with conflicting results. This work was partly motivated by the indications [5] of a zero field hole in the distribution of local fields, $P(h)$, which is often regarded as a signal for spin glass behaviour.

Clearly the behaviour of the entropy as a function of dilution is important for such studies. Exact results are possible for 2D Ising models in the low-temperature limit. We

0305-4470/97/092947+16$19.50

consider the two canonical fully frustrated systems: the Villain model [6] for the square lattice and the triangular antiferromagnet for which the first theoretical work was done by Wannier [7]. Results are presented for both models for the change in entropy due to the presence of a single defect (and as a corollary to terms linear in c for a low concentration, c, of defects). To our knowledge no calculations for the Villain model have appeared previously. There is a single calculation [4] for the triangular antiferromagnet in which the entropy change is related to $P(h = 0)$. In addition we obtain results for the entropy changes that occur due to defect pairs and give the functional dependence on the separation of defects in the pair.

2. Method

The method used in the calculation is based on the combinatorial expansion of the 2D Ising model [8, 9]. This approach has been employed by a number of authors [10–14] to obtain exact results for certain properties of large disordered lattices. The developments described in [10] form the background to the procedure used in this paper; the key points are summarized below.

It is well known [9, 10] that the partition function for 2D Ising systems in the absence of a magnetic field can be expressed as

$$Z = 2^N \left[\prod_{\langle ij \rangle} \cosh(J_{ij}/kT) \right] (\det \mathbf{D})^{1/2} \tag{1}$$

where J_{ij} is the coupling between nearest-neighbour sites i and j, and $\mathbf{D}$ is a matrix whose elements depend on the lattice and are functions of $\{J_{ij}\}$ and temperature T. $\mathbf{D}$ is usually written in a skewed symmetric form, but multiplying all elements by i ($\sqrt{-1}$) does not change the value of the determinant and it does allow us to work with a Hermitian matrix with real eigenvalues.

We showed earlier that this formalism provides a particularly elegant description of the ground-state properties of frustrated systems. Again we can focus on the eigenvalues of $\mathbf{D}$. We can divide the problem into two sets of decoupled eigenstates—those associated with the frustrated plaquettes and the rest. This can be done for frustrated systems generally, but it takes a particularly simple form for the $\pm J$ model (for an arbitrary proportion, p, of $-J$ bonds). In this case (at temperatures near zero) all the frustration eigenvalues can be written as

$$\epsilon = \pm \tfrac{1}{2} X \exp(-2rJ/k_B T) \tag{2}$$

where r is an integer. The number of these eigenstates is precisely equal to the number of frustrated plaquettes. X and r have the physical significance of determining the 'wrong bond' energy, F, and the ground-state entropy, S,

$$F = 2J \sum_d^+ r_d \tag{3}$$

$$S/k_B = \sum_d^+ \ln X_d \tag{4}$$

where the sums are over the frustration states with positive eigenvalues. One can also relate correlation functions to the spatial extent of these frustration states. The fact that F and S are related just to the frustration in the system is intuitively appealing. It should be emphasized, however, that the proof [10] of the apparently simple result in equation (4),

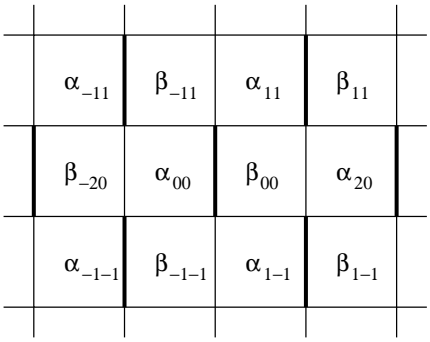

Figure 1. Section of zig-zag domino lattice. Light bonds are positive and heavy ones are negative. Plaquette labelling is shown.

while straightforward, is not trivial. The entropy in equation (4) can alternatively be expressed in terms of the logarithm of a determinant as we shall see later. For the moment, equation (4) conveniently emphasizes the decoupling of eigenstates associated with the frustration.

The approach has already been used [10] to study the $\pm J$ spin glass with $p = 50\%$ and more recently this has been extended to cover the full range of p. The purpose of this paper is to use the formalism in the context of diluted fully frustrated systems. For such systems we have the simplification that we can work just within the subset of frustration states and furthermore all the states are of the type $r = 1$. The following section addresses the Villain model and the subsequent one treats the triangular antiferromagnet.

3. Square lattice

3.1. Villain/zig-zag domino model

The Villain model [6] is a square lattice with every plaquette frustrated. An alternative representation of the fully frustrated square lattice is the zig-zag domino model which is related to the original Villain model by a gauge transformation and is entirely equivalent to it with regards to its properties. In this paper we work with the zig-zag domino representation. The positions of the regularly placed positive and negative bonds are shown in figure 1.

The matrix $\mathbf{D}$ for the square lattice is generally given as follows. Each site is decomposed into four nodes which are connected by a 4×4 block

$$\mathbf{U} = \begin{pmatrix} 0 & -\mathrm{i} & \mathrm{i} & \mathrm{i} \\ \mathrm{i} & 0 & -\mathrm{i} & \mathrm{i} \\ -\mathrm{i} & -\mathrm{i} & 0 & -\mathrm{i} \\ -\mathrm{i} & -\mathrm{i} & \mathrm{i} & 0 \end{pmatrix} \tag{5}$$

on the diagonal of $\mathbf{D}$. The node labelling (see also [10]) is displayed in appendix A. All remaining elements of $\mathbf{D}$ are given by

$$\langle \boldsymbol{i}; 1|\mathbf{D}|\boldsymbol{i} + \hat{\boldsymbol{x}}; 2\rangle = -\mathrm{i}t_{i,i+\hat{x}} \tag{6a}$$

$$\langle \boldsymbol{i}; 3|\mathbf{D}|\boldsymbol{i} + \hat{\boldsymbol{y}}; 4\rangle = -\mathrm{i}t_{i,i+\hat{y}} \tag{6b}$$

where $t_{ij} \tanh(J_{ij}/k_BT)$ and $\hat{\boldsymbol{x}}$ and $\hat{\boldsymbol{y}}$ are unit vectors along the axes of the square lattice.

We may define $\lambda = \frac{1}{4}[1-\tanh(J/k_BT)]$ and write exactly for the fully frustrated system

$$\mathbf{D}(\lambda) = \mathbf{D}(0) + \lambda\mathbf{D}_1 \tag{7}$$

where $\mathbf{D}(0)$ is the zero temperature value of $\mathbf{D}$. The frustration eigenstates, $|f\rangle$, are solutions to $\mathbf{D}(0)|f\rangle = 0$, so that

$$\mathbf{D}|f\rangle = \lambda \mathbf{D}_1|f\rangle. \tag{8}$$

Because there are two plaquettes in each cell of the regular lattice there are two types of state $|f\rangle$ which we denote by $|\alpha\rangle$ (on the left of the negative bond) and $|\beta\rangle$ (on the right of the negative bond). Expressions for these in the node basis are given in appendix A. Plaquette labelling is shown in figure 1.

The next step is to form the matrix $\mathbf{D}_1$ in the basis of these frustrated eigenstates (one for each frustrated plaquette). Because $\lambda \approx \frac{1}{2}\exp(-2J/k_BT)$ at small T, the eigenstates of $\mathbf{D}_1$ provide the coefficients X from which the entropy may be calculated. It should be emphasized at this stage that the entropy depends on $\ln X$. If any of the X's are zero then this simple theory is not valid (it is a flag that states with $r > 1$ are involved). In that case, one would have to return to the theory in the full node basis which is given elsewhere [10]. For the fully frustrated systems, and for the simple defects we shall be considering, none of the X's are zero.

Using the plaquette labelling shown in figure 1, the matrix elements of $\mathbf{D}_1$ are given by

$$\begin{aligned}\langle \alpha_{m,n}|\mathbf{D}_1|\beta_{m',n'}\rangle = \mathrm{i}[&-\delta(m-m')\delta(n-n') + \delta(m-m'-1)\delta(n-n'+1)\\ &+\delta(m-n'-2)\delta(n-n') + \delta(m-m'-1)\delta(n-n'-1)].\end{aligned} \tag{9}$$

The primitive translation vectors are $(2, 0)$ and $(-1, 1)$ and the basic plaquette states are labelled by the unit cell coordinates. The α and β plaquettes are at positions $(-\frac{1}{2}, 0)$ and $(\frac{1}{2}, 0)$ respectively in the unit cell. Making the definition $|\alpha_{\boldsymbol{k}}\rangle = N^{-1/2}\sum_{\boldsymbol{r}} \exp(\mathrm{i}\boldsymbol{k}\cdot\boldsymbol{r})|\alpha_{\boldsymbol{r}}\rangle$ where $\boldsymbol{r} = (m, n) + (-\frac{1}{2}, 0)$ (and similarly for $|\beta_{\boldsymbol{k}}\rangle$), where N is the total number of unit cells (frustrated plaquette pairs), we find that

$$\langle \alpha_{\boldsymbol{k}}|\mathbf{D}_1|\beta_{\boldsymbol{k}'}\rangle = \mathrm{i}2\delta(\boldsymbol{k}-\boldsymbol{k}')(-\mathrm{i}\sin k_x + \cos k_y). \tag{10}$$

It follows that

$$X_k^2 = 4(\sin^2 k_x + \cos^2 k_y). \tag{11}$$

Using equation (4), the entropy per site (the number of plaquette pairs is half the number of sites) is given by

$$S/k_B = \frac{1}{4}\int_0^\pi \frac{\mathrm{d}k_x}{\pi}\int_0^\pi \frac{\mathrm{d}k_y}{\pi}\ln[4(\sin^2 k_x + \cos^2 k_y)] \tag{12}$$

which is the result found by André *et al* [15].

Although this paper is mainly concerned with site dilution, for completeness we will consider a bond defect as well.

3.2. Bond defect

This defect consists of the removal of a single bond rendering unfrustrated regions originally occupied by the associated frustrated plaquette pair. This is displayed in figure 2; the region associated with $|\alpha_{00}\rangle$ and $|\beta_{00}\rangle$ is now unfrustrated. We have the complication of changing the size of the basis. This can easily be dealt with as follows. Apply a perturbation, $\mathbf{V}$, to the $\mathbf{D}_1$ of the perfect system.

$$\mathbf{D}_1 + \mathbf{V} = \begin{pmatrix} \mathbf{d}_I & 0 \\ 0 & \mathbf{d} \end{pmatrix} \tag{13}$$

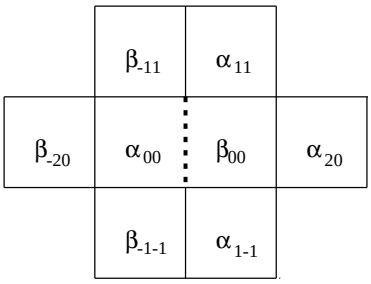

Figure 2. Bond defect (the broken line indicates the bond that is removed). Plaquettes used in the calculation are shown.

where $\mathbf{d}_I$ is the 2×2 block of $\mathbf{D}_1$ associated with α_{00} and β_{00} and $\mathbf{d}$ is the $(N-2)\times(N-2)$ block of $\mathbf{D}_1$ associated with the other plaquettes. $\mathbf{V}$ decouples α_{00} and β_{00} from the rest of the frustrated system. Now if $\mathcal{M}_0$ is the number of ground-state configurations in the fully frustrated system and $\mathcal{M}$ is the quantity for the defective system, we have from equations (2) and (4), $\mathcal{M}_0^2 = |\mathbf{D}_1|$ and $\mathcal{M}^2 = |\mathbf{d}|$. It follows immediately that

$$\mathcal{M}^2 = \frac{\mathcal{M}_0^2 |\boldsymbol{I} + \mathbf{D}_1^{-1}\mathbf{V}|}{|\boldsymbol{d}_I|}. \tag{14}$$

Now there are only non-zero matrix elements between $|\alpha\rangle$ and $|\beta\rangle$ states so that it is convenient to define

$$\langle \alpha_{i+m,j+n} | \mathbf{D}_1^{-1} | \beta_{i,j} \rangle = \mathrm{i} g_{mn} \tag{15a}$$

$$\langle \beta_{i+m,j+n} | \mathbf{V} | \alpha_{i,j} \rangle = \mathrm{i} v_{mn} \tag{15b}$$

$$\langle \alpha_{i+m,j+n} | \boldsymbol{d}_I | \beta_{i,j} \rangle = \mathrm{i} d'_{mn}. \tag{15c}$$

Each determinant in equation (14) becomes the product of identical determinants and we can write

$$\mathcal{M} = \frac{\mathcal{M}_0 |I - \mathbf{gv}|}{|\boldsymbol{d}'|} \tag{16}$$

where it is understood that it is the magnitude of the determinants that we take. The change in entropy from the fully frustrated value is given by

$$\Delta S / k_B = \ln |I - \mathbf{gv}| - \ln |\boldsymbol{d}'|. \tag{17}$$

An identical formalism will be employed for the more complex defect structures studied later in this paper. In general, the defect cluster comprises n frustrated plaquettes; $\mathbf{d}_I$ and $\mathbf{d}$ are $n\times n$ and $(N-n)\times(N-n)$ blocks respectively. $\mathbf{D}_1^{-1}$ and $\mathbf{V}$ are $n_v \times n_v$ blocks, where n_v is the sum of n and the number of plaquette states that are coupled to the defect cluster by elements of $\mathbf{D}_1$. $(I-\mathbf{gv})$ comprises two diagonal blocks of the order of $n_v/2$, one associated with the α states and the other with the β states. It is to be understood that the determinant in equation (16) is of just one of these blocks. Similarly $\mathbf{d}'$ also comprises two blocks of the order of $n_v/2$, but in this case they are off-diagonal blocks. Again the determinant of just one block is understood in equation (16). $\mathbf{g}$ and $\mathbf{v}$ also comprise off-diagonal blocks.

For the bond defect ($n_v = 8$; see figure 2), the decoupling matrix $\mathbf{v}$ is given by

$$\mathbf{v} = \begin{pmatrix} 0 & 1 & 1 & 1 \\ 1 & 0 & 0 & 0 \\ 1 & 0 & 0 & 0 \\ 1 & 0 & 0 & 0 \end{pmatrix}. \tag{18}$$

Rows and columns of the full 8×8 matrix are ordered: $|\alpha_{00}\rangle$, $|\alpha_{11}\rangle$, $|\alpha_{1-1}\rangle$, $|\alpha_{20}\rangle$, $|\beta_{00}\rangle$, $|\beta_{-11}\rangle$, $|\beta_{-1-1}\rangle$, $|\beta_{-20}\rangle$. Equation (18) represents the lower left off-diagonal block.

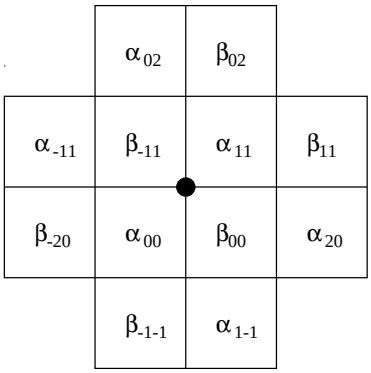

Figure 3. Site defect (bonds connected to heavy dot are removed). Plaquettes shown are the ones involved in the calculation.

The elements of **g** are found in the usual way

$$g_{mn} = \frac{1}{2}\int_{-\pi/2}^{\pi/2}\frac{\mathrm{d}k_y}{\pi}\int_{-\pi}^{\pi}\frac{\mathrm{d}k_y}{2\pi}\frac{\exp[\mathrm{i}k_x(m-1)]\cos nk_y}{\mathrm{i}\sin k_x + \cos k_y}. \tag{19}$$

Equation (19) relates to the upper right off-diagonal block (see equation (15*a*)). There are a number of symmetry relations and sum rules; these are given in appendix C together with a selection of values of matrix elements. The determinants in equation (16) are easily evaluated. $|I - \mathbf{gv}|$ is just $\frac{1}{4}$ and the denominator is unity (there is no entropy associated with the isolated defect), so that $\mathcal{M} = \mathcal{M}_0/4$ and, for a low concentration, c, of such defects, the entropy shift is given by

$$\Delta S/k_B = -2c\ln 4. \tag{20}$$

The factor of 2 appears because we evaluate the entropy per site and c is the fraction of removed bonds (N sites and $2N$ bonds). The result can also be easily obtained from a symmetry argument. If we focus on, say, the α_{00} plaquette in figure 2 then, in the perfect lattice, $\frac{1}{4}$ of the ground-state configurations have the wrong bond on the negative bond between α_{00} and β_{00}. When the defect is present, this bond is removed and so those configurations have lower energy (the new ground states). This is the origin of the factor of $\frac{1}{4}$. Although the result is a trivial one, it does provide a simple illustration of the method prior to considering more complex situations.

3.3. Site defect

The site defect involves the removal of all bonds connected to a particular site. The group of plaquettes that we need to consider is shown in figure 3. The unfrustrated region now is that associated with α_{00}, α_{11}, β_{00}, β_{-11} (n is now 4). This situation can be treated in a similar way to the bond defect. Again a decoupling term, **V**, is defined. Now n_v is 12 and **v** (from equation (15*b*)) is the following 6×6 block

$$\mathbf{v} = \begin{pmatrix} 0 & 0 & 1 & 1 & 0 & 0 \\ 0 & 0 & 0 & 0 & -1 & 1 \\ 1 & 0 & 0 & 0 & 0 & 0 \\ 1 & 0 & 0 & 0 & 0 & 0 \\ 0 & -1 & 0 & 0 & 0 & 0 \\ 0 & 1 & 0 & 0 & 0 & 0 \end{pmatrix}. \tag{21}$$

The basis states are ordered $|\alpha_{00}\rangle$, $|\alpha_{11}\rangle$, $|\alpha_{1-1}\rangle$, $|\alpha_{20}\rangle$, $|\alpha_{-11}\rangle$, $|\alpha_{02}\rangle$, $|\beta_{00}\rangle$, $|\beta_{-11}\rangle$, $|\beta_{-1-1}\rangle$, $|\beta_{-20}\rangle$, $|\beta_{11}\rangle$, $|\beta_{02}\rangle$.

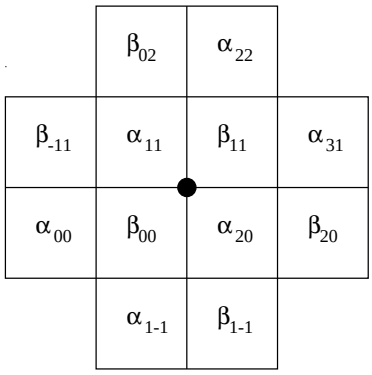

Figure 4. Site defect; the alternative one to the one shown in figure 3.

Again we use equation (16). There is considerable simplification if we use the sum rule in appendix C. The determinant $|I - \mathbf{gv}|$ easily reduces to $2(g_{11}g_{1-1} - g_{00}g_{20})$, and $|\mathbf{d}'|$ is 2, so that $\mathcal{M} = \mathcal{M}_0/8$ and, for a low concentration, c, of site defects, the entropy shift is given by

$$\Delta S/k_B = -c \ln 8. \tag{22}$$

Although one could have anticipated the fact that the entropy shift due to the bond defect can be expressed in terms of a simple integer, the similar simplicity for the site defect is perhaps a little surprising; certainly it does not happen for the site defect in the triangular antiferromagnet (see section 4). It is interesting therefore to explore the situation when more than one defect is present.

3.4. Site defect pairs (non-overlapping)

We consider the effect on the entropy due to the presence of a pair of *non-overlapping* site defects. The first defect is based on plaquettes α_{00}, β_{00}, α_{11}, β_{-11} as in figure 3. For the second defect there are two distinct cases: either it is based on $\alpha_{M+0,N+0}$, $\beta_{M+0,N+0}$, $\alpha_{M+1,N+1}$, $\beta_{M-1,N+1}$ (i.e. as in figure 3 but shifted by M, N), or it is based on $\beta_{M+0,N+0}$, $\alpha_{M+2,N+0}$, $\beta_{M+1,N+1}$, $\alpha_{M+1,N+1}$ (as in figure 4 with a shift by M, N). We shall call these cases (i) and (ii) respectively. To make the results clearer, it is convenient to introduce indices (μ, ν) to represent the separation of the site defects; (M, N) are unit cell separations. The relations between the two are: for case (i), $\mu = M$, $\nu = N$; for case (ii), $\mu = M + 1$, $\nu = N$.

3.4.1. Case (i) ($\mu + \nu$ even). Much of the simplification that arose in the analysis of the single defect case stemmed from the use of the sum rule and the symmetry relations. A similar simplification occurs here as well. For compactness of notation, we define $g^{\pm}_{mn} = g_{\pm M+m,\pm N+n}$. There is a $|\mathbf{d}'|$ associated with each defect independently which immediately gives a factor of 4 in the denominator of equation (16). Now $n_v = 24$ and the decoupling matrix, $\mathbf{v}$, is of size 12×12 (two 6×6 blocks, one associated with each defect). Using the sum rule in appendix C, the 12×12 determinant $|I - \mathbf{gv}|$ is easily reduced to a smaller one so that we can write

$$\frac{\mathcal{M}}{\mathcal{M}_0} = \begin{vmatrix} g_{00} & g_{1-1} & g^{-}_{00} & g^{-}_{1-1} \\ g_{11} & g_{20} & g^{-}_{11} & g^{-}_{20} \\ g^{+}_{00} & g^{+}_{1-1} & g_{00} & g_{1-1} \\ g^{+}_{11} & g^{+}_{20} & g_{11} & g_{20} \end{vmatrix}. \tag{23}$$

The upper-left and lower-right 2×2 blocks are the single defect contributions; the off-diagonal blocks represent pair effects. The symmetry relations in appendix C can be used to show that

$$g^{-}_{00} = \pm g^{+}_{20} \tag{24a}$$

$$g^{-}_{20} = \pm g^{+}_{00} \tag{24b}$$

$$g^{-}_{1\pm1} = \mp g^{+}_{1\mp1} \tag{24c}$$

where the $\pm$ signs prefixing the g refer to M, N odd (upper sign) or even (lower). We can pull out the single defect contributions as a prefactor and write

$$\frac{\mathcal{M}}{\mathcal{M}_0} = \frac{1}{8^2}\begin{vmatrix} 1 & 0 & \mp 2(g^{+}_{1-1} + g^{+}_{20}) & \pm 2(g^{+}_{00} + g^{+}_{11}) \\ 0 & 1 & \mp 2(g^{+}_{1-1} - g^{+}_{20}) & \pm 2(g^{+}_{00} - g^{+}_{11}) \\ 2(-g^{+}_{00} + g^{+}_{11}) & 2(-g^{+}_{1-1} + g^{+}_{20}) & 1 & 0 \\ 2(g^{+}_{00} + g^{+}_{11}) & 2(g^{+}_{1-1} + g^{+}_{20}) & 0 & 1 \end{vmatrix}. \tag{25}$$

Evaluating the determinant yields

$$\frac{\mathcal{M}}{\mathcal{M}_0} = \frac{1}{8^2}[1 \mp 8\{(g^{+}_{00})^2 + (g^{+}_{11})^2 + (g^{+}_{1-1})^2 + (g^{+}_{20})^2\} + 64\{g^{+}_{00}g^{+}_{20} - g^{+}_{11}g^{+}_{1-1}\}^2]. \tag{26}$$

The prefactor 8^{-2} is the contribution from the two defects independently (see equation (22)), and the term in the square brackets gives the pair effect. The asymptotic behaviour of the functions in equation (26) can be found for large impurity separation (see appendix C for the elements of g). The following configurations are considered: $(\mu = R, \nu \ll \mu)$; $(\mu \ll \nu, \nu = R)$; $(\mu = \nu = R)$. In each case, equation (26) yields to the leading term in R^{-1}

$$\frac{\mathcal{M}}{\mathcal{M}_0} = \frac{1}{8^2}\left[1 + A(-1)^R \frac{16}{\pi^2 R^2}\right] \tag{27}$$

where $A = 1$ for the first two defect configurations and $A = \frac{1}{2}$ if they lie along a diagonal.

3.4.2. Case (ii) ($\mu + \nu$ odd). We follow the procedure described for the previous case. The expression equivalent to equation (23) is

$$\frac{\mathcal{M}}{\mathcal{M}_0} = \begin{vmatrix} g_{00} & g_{1-1} & g^{-}_{00} & g^{-}_{-1-1} \\ g_{11} & g_{20} & g^{-}_{11} & g^{-}_{00} \\ g^{+}_{20} & g^{+}_{3-1} & g_{20} & g_{1-1} \\ g^{+}_{11} & g^{+}_{20} & g_{11} & g_{00} \end{vmatrix}. \tag{28}$$

Again we employ similar symmetry relations, and obtain as the expression that is the counterpart of equation (26)

$$\frac{\mathcal{M}}{\mathcal{M}_0} = \frac{1}{8^2}[1 \pm 4\{2g^{+}_{20}(g^{+}_{11} + g^{+}_{1-1} - g^{+}_{31} - g^{+}_{3-1}) + (g^{+}_{11} + g^{+}_{3-1})(g^{+}_{1-1} + g^{+}_{31})\} + 64\{(g^{+}_{20})^2 - g^{+}_{11}g^{+}_{3-1}\}\{(g^{+}_{20})^2 - g^{+}_{1-1}g^{+}_{31}\}]. \tag{29}$$

Referring to the elements of g listed in appendix C, we find that the $O(R^{-2})$ corrections to the independent defect behaviour are zero in this case. The leading corrections are $O(R^{-4})$. The final term in equation (29) is clearly of this order. There is also a contribution from the other term in equation (29) for which it was necessary to expand elements of g to $O(R^{-2})$. The result for $(\mu = R, \nu \ll \mu)$ and $(\mu \ll \nu, \nu = R)$ is

$$\frac{\mathcal{M}}{\mathcal{M}_0} = \frac{1}{8^2}\left[1 - \frac{16(B\pi^2 - 4)}{\pi^4 R^4}\right] \tag{30}$$

where, for the $\nu \gg \mu$ regime, $B = 5$ if μ is even and ν is odd, and $B = 1$ if μ is odd and ν is even. For $\mu \gg \nu$, the values of B are reversed in accordance with the symmetry of the square lattice. The diagonal configuration is always case (i).

3.4.3. Comments. The entropy shift for large R can then be written as

$$\Delta S/k_B = -2\ln 8 + 16A(-1)^R/(\pi R)^2 \tag{31a}$$

if $\mu + \nu$ is even and, if it is odd, as

$$\Delta S/k_B = -2\ln 8 - 16(B\pi^2 - 4)/(\pi R)^4. \tag{31b}$$

It is interesting to compare the behaviour of the pair corrections with the correlation functions that have been calculated [16–18] for this model. Clearly the two are related, albeit rather indirectly. It should be noted that the pair corrections in this entropy calculation, unlike the correlation functions, do not depend on the particular gauge used. The correlation functions can oscillate with a period of 2 or 4 with a distance [18] depending on the gauge (Villain or zig-zag domino). Diagonal correlations oscillate between zero and a finite value (which can be positive or negative in the gauge that displays a period of 4); the corresponding pair entropy corrections in equation (27) oscillate between positive and negative values with a period of 2.

Now specifically consider defects lying along the vertical ($\mu = 0$) or horizontal axes ($\nu = 0$) for which R is even (case (i)) or odd (case (ii)). Pair corrections to the entropy now oscillate with a period of 2 between $O(R^{-2})$ and $O(R^{-4})$ behaviour, whereas the correlations [18] vary between two non-zero values while maintaining the $R^{-1/2}$ dependence that characterizes the correlation functions of the fully frustrated systems.

It is worth noting that the asymptotic elements of g listed in appendix C depend on the particular gauge used and are not expected to exhibit the symmetry of the lattice. The entropy changes, of course, are identical for symmetrically equivalent defect configurations.

4. Triangular lattice

4.1. Fully frustrated antiferromagnet

The fully frustrated triangular lattice can be realized by placing negative antiferromagnetic bonds everywhere. The matrix $\mathbf{D}$ for the triangular lattice [9] has diagonal blocks linking six nodes per site and other elements analogous to those for the zig-zag domino model. Again we can develop the discussion in terms of eigenstates associated with the frustrated plaquettes. Equations (2) and (4) still apply apart from a prefactor of $\frac{2}{3}$:

$$\epsilon = \pm\tfrac{2}{3}X\exp(-2rJ/k_BT). \tag{32}$$

The relation between the frustrated plaquette and the node basis is given in appendix B. So that equations (12)–(14) are still applicable, we will write $\mathbf{D}_1$ as in equation (7) but with λ now defined as

$$\lambda = \tfrac{1}{3}[1 - \tanh(J/k_BT)] \tag{33}$$

The labelling for the frustrated plaquette basis is shown in figure 5. In the diagrams we represent the triangular lattice as the topologically equivalent square lattice with bonds across one diagonal. The matrix elements of $\mathbf{D}_1$ are all given by

$$\langle\alpha|\mathbf{D}_1|\beta\rangle = \mathrm{i} \tag{34}$$

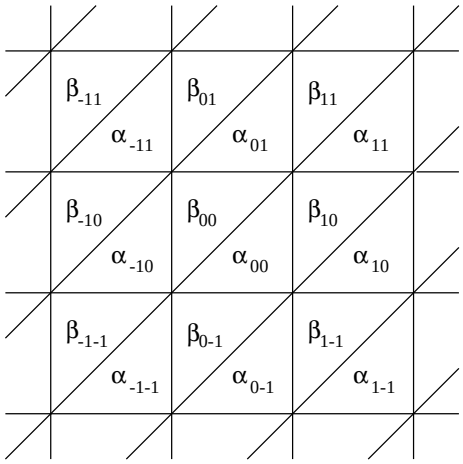

Figure 5. Section of triangular antiferromagnet. All bonds are negative. Plaquette labelling is shown.

so that

$$\langle\alpha_{m,n}|\mathbf{D}_1|\beta_{m,n'}\rangle = \mathrm{i}[\delta(m-m')\delta(n-n') + \delta(m-m'+1)(\delta(n-n') + \delta(m-m')\delta(n-n'-1)]. \tag{35}$$

The Fourier transformation then yields

$$\langle\alpha_{\boldsymbol{k}}|\mathbf{D}_1|\beta_{\boldsymbol{k}'}\rangle = \mathrm{i}\delta(\boldsymbol{k}-\boldsymbol{k}')[1+\exp(\mathrm{i}k_x)+\exp(-\mathrm{i}k_y)] \tag{36}$$

and

$$X_k^2 = 3 + 2[\cos k_x + \cos k_y + \cos(k_x + k_y)]. \tag{37}$$

The entropy is then

$$S/k_B = \frac{1}{2}\int_0^\pi \frac{\mathrm{d}k_x}{\pi}\int_0^\pi \frac{\mathrm{d}k_y}{\pi}\ln[3 + 2(\cos k_x + \cos k_y + \cos(k_x + k_y))] \tag{38}$$

which can be shown to agree with the result of Wannier [7].

4.2. Bond defect

The procedure closely follows that of section 2. We define $\mathbf{g}$, $\mathbf{v}$, and $\mathbf{d}'$ as in equation (15) and then employ equations (16) and (17) to find the entropy changes. The notation for the bond defect is shown in figure 6 and, with basis states ($n_v = 6$) ordered $|\alpha_{00}\rangle$, $|\alpha_{10}\rangle$, $|\alpha_{11}\rangle$, $|\beta_{10}\rangle$, $|\beta_{00}\rangle$, $|\beta_{0-1}\rangle$, the decoupling matrix is

$$\mathbf{v} = \begin{pmatrix} 0 & 1 & 1 \\ 1 & 0 & 0 \\ 1 & 0 & 0 \end{pmatrix} \tag{39}$$

and

$$g_{mn} = \int_{-\pi}^{\pi}\frac{\mathrm{d}k_x}{2\pi}\int_{-\pi}^{\pi}\frac{\mathrm{d}k_y}{2\pi}\frac{\cos[mk_x + nk_y] + \cos[(m+1)k_x + nk_y] + \cos[mk_x + (n-1)k_y]}{3 + 2[\cos k_x + \cos k_y + \cos(k_x + k_y)]}. \tag{40}$$

The symmetry relation and sum rule for the triangular antiferromagnet are given in appendix D together with a selection of values of matrix elements. The determinants in equation (16) are easily evaluated. $|I - \mathbf{gv}|$ is just $\frac{1}{3}$ and the denominator is unity (there

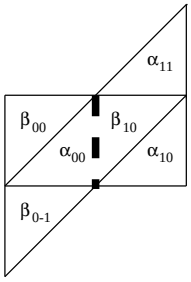

Figure 6. Bond defect. The broken line indicates the bond that is removed. Plaquettes relevant to the calculation are shown.

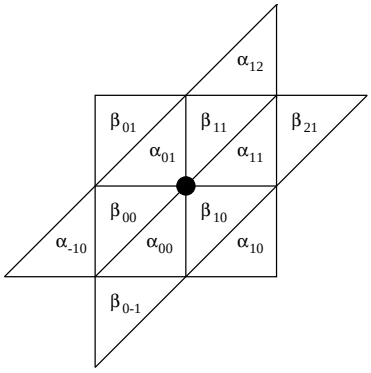

Figure 7. Site defect. Bonds connected to the heavy dot are removed. Relevant plaquettes are shown.

is no entropy associated with the isolated defect), so that $\mathcal{M} = \mathcal{M}_0/3$ and, for a low concentration, c, of such defects, the entropy shift is given by

$$\Delta S/k_B = -3c \ln 3. \tag{41}$$

The prefactor of 3 appears because there are three bonds per site. As in the case of the square lattice, this result could be anticipated by symmetry arguments.

4.3. Site defect

The notation for the site defect in the triangular antiferromagnet is shown in figure 7. The decoupling matrix ($n_v = 12$) is

$$\mathbf{v} = \begin{pmatrix} 0 & 0 & 0 & 1 & 0 & 0 \\ 0 & 0 & 0 & 0 & 1 & 0 \\ 0 & 0 & 0 & 0 & 0 & 1 \\ 1 & 0 & 0 & 0 & 0 & 0 \\ 0 & 1 & 0 & 0 & 0 & 0 \\ 0 & 0 & 1 & 0 & 0 & 0 \end{pmatrix} \tag{42}$$

with basis states ordered $|\alpha_{01}\rangle$, $|\alpha_{11}\rangle$, $|\alpha_{00}\rangle$, $|\alpha_{10}\rangle$, $|\alpha_{12}\rangle$, $|\alpha_{-10}\rangle$, $|\beta_{10}\rangle$, $|\beta_{11}\rangle$, $|\beta_{00}\rangle$, $|\beta_{01}\rangle$, $|\beta_{21}\rangle$, $|\beta_{0-1}\rangle$.

The sum rule and symmetry relations (see appendix D) can again be used to give considerable simplification. The determinant $|I - \mathbf{gv}|$ can be reduced to $2(g_{00} - g_{-11})^2(2g_{00} + g_{-11})$ and $|\mathbf{d}'|$ is 2, so that, for a low concentration, c, of site defects, the entropy shift is given by

$$\Delta S/k_B = c \ln \left[\left(\frac{1}{3} + \frac{\sqrt{3}}{2\pi} \right)^2 \left(\frac{2}{3} - \frac{\sqrt{3}}{2\pi} \right) \right] \tag{43}$$

or

$$\Delta S/k_B = -c1.9309. \tag{44}$$

This is the first direct derivation of this result that we are aware of. Farach *et al* [4] used an alternative approach and obtained the expression

$$\Delta S/k_B = c[\ln 2 - \ln P(0)] \tag{45}$$

where $P(h)$ is the distribution function for local fields in a triangular antiferromagnet. Choy and Sherrington [19] obtained a numerical value for $P(0)$ which when substituted into equation (45) reproduced the result in equations (43), (44). There appears to be an error in the numerical result quoted by Farach *et al* [4].

4.4. Site defect pairs (non-overlapping)

For a pair of non-overlapping site defects we can proceed in a fashion similar to that used for the square lattice in section 2.4. A similar notation, $g^{\pm}_{mn} = g_{\pm M+m,\pm N+n}$, is used. Again we are dealing with a 12×12 determinant ($n_v = 24$); in this case it can be reduced by using the sum rules to a simpler form.

$$\frac{\mathcal{M}}{\mathcal{M}_0} = \begin{vmatrix} g_{-11} & g_{-10} & g_{01} & g^{-}_{-11} & g^{-}_{-10} & g^{-}_{01} \\ g_{01} & g_{00} & g_{11} & g^{-}_{01} & g^{-}_{00} & g^{-}_{11} \\ g_{-10} & g_{-1-1} & g_{00} & g^{-}_{-10} & g^{-}_{-1-1} & g^{-}_{00} \\ g^{+}_{-11} & g^{+}_{-10} & g^{+}_{01} & g_{-11} & g_{-10} & g_{01} \\ g^{+}_{01} & g^{+}_{00} & g^{+}_{11} & g_{01} & g_{00} & g_{11} \\ g^{+}_{-10} & g^{+}_{-1-1} & g^{+}_{00} & g_{-10} & g_{-1-1} & g_{00} \end{vmatrix}. \tag{46}$$

The diagonal 3×3 blocks are the contributions from isolated defects and, if the off-diagonal blocks were neglected and symmetry relations ($g_{-10} = g_{01} = g_{00}$; $g_{11} = g_{-1-1} = g_{-11}$) were used, we would retrieve equation (43). There does not appear to be any further simplification in the general case, but we will evaluate the asymptotic behaviour for the case ($M = R, N = R$). For this case the lower left-hand 3×3 block in equation (46) is the transpose of the upper right-hand block. Furthermore, from the symmetry of the six-fold symmetry of the triangular lattice, the determinant in equation (46) has the same value for $(M, N) = (R, R); (-R, -R); (R, 0); (-R, 0); (0, R); (0, -R)$. This can be confirmed via the symmetry relations obeyed by the g's that are given in appendix D.

Using the asymptotic forms for the set of g's listed in appendix D, equation (46) can be evaluated analytically to leading order in R^{-1}

$$\frac{\mathcal{M}}{\mathcal{M}_0} = \left[\left(\frac{1}{3} + \frac{\sqrt{3}}{2\pi}\right)^2 \left(\frac{2}{3} - \frac{\sqrt{3}}{2\pi}\right)\right]^2 \left[1 + \frac{9\sigma}{2\pi^2\xi^2R^2}\right] \tag{47}$$

where

$$\xi = \frac{1}{3} + \frac{\sqrt{3}}{2\pi} \tag{48}$$

and σ is 1 if $R = 3 \times$ integer and $-\frac{1}{2}$ otherwise.

As with the square lattice, it is interesting to make comparisons with the correlation functions. Both the pair corrections to the entropy and the correlations [20] exhibit oscillations with a period of 3. Furthermore, the numerical factor appearing in the correlation functions shows a sublattice dependence [20] that exactly matches that shown here by σ.

The entropy shift for large R can be written as

$$\Delta S/k_B = 2\ln\left[\left(\frac{1}{3} + \frac{\sqrt{3}}{2\pi}\right)^2 \left(\frac{2}{3} - \frac{\sqrt{3}}{2\pi}\right)\right] + 9\sigma/[2(\pi\xi R)^2]. \tag{49}$$

5. Conclusions

We have evaluated the entropy shift due to some defect configurations in two fully frustrated systems. For the bond defects, the results are simple and could be obtained equally by symmetry arguments. However, they are useful for illustrating the method. The more physically interesting site defects give non-trivial results. Although the site defect in the square lattice does produce a simple expression (equation (22)), we are unable to reproduce it by the kind of symmetry arguments applicable for bond defects. For a finite concentration, c, of defects, the single defect results, of course, also provide the leading term in an expansion in powers of c.

Pair effects are also considered for site defects. In both systems, pair corrections are of the order of R^{-2} (or R^{-4} for certain values of R in the square lattice), where R is the separation of the members of the pair. Representative configurations are examined. We could, in principle, develop this study to obtain $O(c^2)$ terms. This would require a numerical evaluation and a summation over relative positions of defects. It is likely that the summation would be fairly rapidly convergent.

A more profitable objective would be the exact evaluation of the ground-state entropy over a wide range of c (from zero to the percolation threshold) and averaging the entropy over a large sample of defect configurations. This approach has already been employed [10] for the $\pm J$ model. The methods [10, 12–14] that allow an exact calculation of the ground-state properties provide an important complement to the Monte Carlo simulations which are particularly difficult to apply to frustrated systems in the low-temperature limit.

Acknowledgment

One of us (JRG) acknowledges the support of the Brazilian agency CNPq.

Appendix A

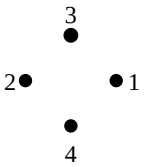

Figure A1. Node labelling for square lattice.

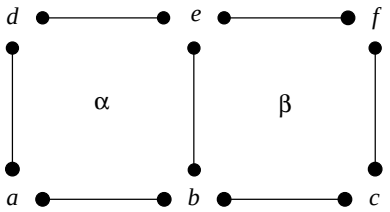

Figure A2. Nodes required to define plaquette states $|\alpha\rangle$ and $|\beta\rangle$ for zig-zag domino model.

The original node basis for the square lattice (see [10]) is defined in figure A1. For the zig-zag domino model the two types of frustrated plaquette are shown in figure A2. The relation between the node and the frustrated plaquette basis is

$$|\alpha = \frac{1}{\sqrt{8}}[|a,3\rangle + |a,1\rangle - |d,4\rangle + |d,1\rangle - |e,2\rangle - |e,4\rangle + |b,3\rangle + |b,2\rangle] \tag{A1}$$

$$|\beta = \frac{1}{\sqrt{8}}[|b,3\rangle + |b,1\rangle + |e,4\rangle - |e,1\rangle + |f,2\rangle + |f,4\rangle + |c,3\rangle + |c,2\rangle]. \tag{A2}$$

Appendix B

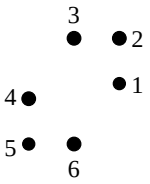

Figure B1. Node labelling for triangular lattice.

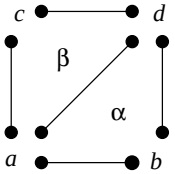

Figure B2. A representation of the nodes required to define plaquette states $|\alpha\rangle$ and $|\beta\rangle$ for triangular antiferromagnet.

The original node basis for the triangular lattice (see [9]) is defined in figure B1. For the triangular antiferromagnet the two types of frustrated plaquette are shown in figure B2. The relation between the node and the frustrated plaquette basis is

$$|\alpha = \frac{1}{\sqrt{6}}[|a,1\rangle + |a,2\rangle + |d,5\rangle + |d,6\rangle - |b,3\rangle - |b,4\rangle] \tag{B1}$$

$$|\beta = \frac{1}{\sqrt{6}}[|a,2\rangle + |a,3\rangle - |d,4\rangle - |d,5\rangle - |c,1\rangle + |c,6\rangle]. \tag{B2}$$

Appendix C

The following sum rule and symmetry relations for the elements of g for the zig-zag domino model exist

$$g_{m,n} = g_{m,-n} \tag{C1}$$

$$g_{m,n} = \pm g_{2-m,n}. \tag{C2}$$

The $\pm$ signs in equation (C2) refer to m and n odd/even.

$$g_{m,n} = (-1)^{(m+n+2)/2} g_{n+1,m-1} \tag{C3}$$

$$-g_{m,n} + g_{m+1,n-1} + g_{m+1,n+1} + g_{m+2,n} = \delta_{m0}\delta_{n0}. \tag{C4}$$

Selected elements of g (see equation (19)) are evaluated as follows

m	n	g_{mn}
0	0	$-\frac{1}{4}$
1	± 1	$\frac{1}{4}$
2	0	$\frac{1}{4}$
-1	± 1	$1/\pi - \frac{1}{4}$
0	± 2	$1/\pi - \frac{1}{4}$.

Asymptotic expressions for the elements of g are required to progress from equation (26) to equation (27) and from equation (29) to equation (30). A single integration in equation (19) followed by an integration by parts leads to the following expressions taken to $O(R^{-2})$. For $M \gg N$:

$$g^{+}_{mn} = \frac{(-1)^{(N+n)/2}}{\pi(M+m-1)} \tag{C5}$$

if $N+n$ is even, and

$$g^{+}_{mn} = \frac{(-1)^{(N+n)/2}(N+n)}{\pi(M+m-1)^2} \tag{C6}$$

if $N+n$ is odd.

For $N \gg M$:

$$g^{+}_{mn} = \frac{(-1)^{(N+n)/2}}{\pi(N+n)} \tag{C7}$$

if $M+m$ is odd, and

$$g^{+}_{mn} = \frac{(M+m-1)(-1)^{(N+n)/2}}{\pi(N+n)^2} \tag{C8}$$

if $N+n$ is even.

For $M=N=R$:

$$g^{+}_{mn} = \frac{(-1)^{(R+n)/2}}{2\pi R} \tag{C9}$$

if $M+m$ and $N+n$ are even, and

$$g^{+}_{mn} = \frac{(-1)^{(R+n-1)/2}}{2\pi R} \tag{C10}$$

if $M+m$ and $N+n$ are odd. Otherwise this quantity is zero.

The sum rule, equation (C3), is satisfied to $O(R^{-2})$ for the $M \gg N$ and $N \gg M$ cases, and to $O(R^{-1})$ for $M=N$.

Appendix D

The following sum rule and symmetry relations for the elements of g for the triangular antiferromagnet exist

$$g_{m,n} = g_{-n,-m} \tag{D1}$$

$$g_{m,n} + g_{m-1,n} + g_{m,n+1} = \delta_{m0}\delta_{n0} \tag{D2}$$

$$g_{m,m+p} = g_{m,1-p}. \tag{D3}$$

If values of $g_{m,-m}$ are known for integer values of m, all other elements can be obtained from equations (D1) and (D2). The $g_{m,-m}$ that are required for this paper are evaluated from equation (39) and are listed below

m	n	g_{mn}
0	0	$\frac{1}{3}$
-1	1	$-\sqrt{3}/2\pi$
1	-1	$-\sqrt{3}/\pi + \frac{2}{3}$.

Asymptotic expressions for the elements of g required in the derivation of equation (46) can be obtained in the manner used in appendix C. For $M=N=R$ and to the leading order in R^{-1}, it can be shown that

$$g^{+}_{mn} = -\frac{(-1)^{m-n}}{\pi R}\sin[\pi(2R+m+n)/3]. \tag{D4}$$

Equation (D2) is satisfied to $O(R^{-1})$.

References

[1] Grest G S and Gabl E G 1979 *Phys. Rev. Lett.* **43** 1182
[2] Blackman J A, Kemeny G and Straley J P 1981 *J. Phys. C: Solid State Phys.* **14** 385
[3] Andérico C Z, Fernández J F and Streit T S J 1982 *Phys. Rev.* B **26** 3824
[4] Farach H A, Creswick R J and Poole C P 1988 *Phys. Rev.* B **37** 5615
[5] Creswick R J, Farach H A, Poole C P and Knight J M 1985 *Phys. Rev.* B **32** 5776
[6] Villain J 1977 *J. Phys. C: Solid State Phys.* **10** 1717
[7] Wannier G H 1950 *Phys. Rev.* **79** 357
Wannier G H 1973 *Phys. Rev.* B **7** 5017
[8] Kac M and Ward J C 1952 *Phys. Rev.* **88** 1332
[9] Green H S and Hurst C A 1964 *Order–Disorder Phenomena* (London: Interscience)
[10] Blackman J A and Poulter J 1991 *Phys. Rev.* B **44** 4374
[11] Blackman J A 1982 *Phys. Rev.* B **26** 4987
[12] Inoue M 1995 *J. Phys. Soc. Japan* **64** 3699
[13] Saul L and Kardar M 1993 *Phys. Rev.* E **48** R3221
[14] Saul L and Kardar M 1994 *Nucl. Phys.* B **432** 641
[15] André G, Bidaux R, Carton J P, Conte R and de Seze L 1979 *J. Physique* **40** 479
[16] Forgacs G 1980 *Phys. Rev.* B **22** 4473
[17] Gabay M 1980 *J. Phys. Lett.* **41** 427
[18] Wolff W F and Zittartz J 1982 *Z. Phys.* B **47** 341
[19] Choy T C and Sherrington D 1983 *J. Phys. A: Math. Gen.* **16** L265
Choy T C and Sherrington D 1983 *J. Phys. A: Math. Gen.* **16** 3691
[20] Stephenson J 1970 *J. Math. Phys.* **11** 413